Research Article

Synthesis and Antibacterial Activity of Polyoxometalates with Different Structures

Jingmin Gu [1], **Lei Zhang,**[2] **Xiaofeng Yuan,**[3] **Ya-Guang Chen** [4] **Xiuzhu Gao,**[5] **and Dong Li** [5,6]

[1]*College of Veterinary Medicine, Jilin University, Changchun 130062, China*
[2]*Animal Science and Technology College, Jilin Agricultural University, Changchun 130117, China*
[3]*Department of Pediatrics, Affiliated Hospital of the Changchun University of Chinese Medicine, Changchun 130021, China*
[4]*Key Laboratory of Polyoxometalates Science of Ministry of Education, Faculty of Chemistry, Northeast Normal University, Changchun 130024, China*
[5]*Department of Hepatology, The First Hospital, Jilin University, Changchun 130021, China*
[6]*Department of Immunology, College of Basic Medical Sciences, Jilin University, Changchun 130021, China*

Correspondence should be addressed to Dong Li; lidong1@jlu.edu.cn

A new inorganic-organic hybrid compound, $[\{Cu(phen)_2\}_2(H_4W_{12}O_{40})]$, was synthesized, and its crystal structure was determined. The Keggin anion $H_4W_{12}O_{40}{}^{4-}$ was grafted with two coordination units $\{Cu(phen)_2\}$, forming an electrically neutral molecule. The antibacterial activity of several polyoxometalate compounds with different anionic structures including the new compound was studied. The results show that the compound **1** can inhibit the growth of *Enterococcus faecalis* FA2 strains and that antibacterial activity of the polyoxometalate compounds is dependent with component elements of POM but is less relative with the anion structures.

1. Instruction

Polyoxometalates (POMs) have been shown to exhibit biological activities *in vitro* as well as *in vivo*, including anticancer and antiviral [1], antibacterial [2, 3], antiprotozoal [4, 5], and antidiabetic activities [6]. In the antibacterial activity study of POMs, Tajima found the enhancement of several beta-lactams antibiotics in antibacterial activity to methicillin-resistant *Staphylococcus aureus* under the synergistic action of polyoxometalates, substituted-type POMs $K_7[PTi_2W_{10}O_{40}]$ $6H_2O$, $K_7[BVW_{11}O_{40}]7H_2O$, $[SiFeW_{11}O_{40}]^{6/5-}$ and $[SiCoW_{11}O_{40}]^{6-}$ and lacunary-type POMs $[XW_{11}O_{39}]^{n-}$ (X = Si, P) and $[XW_9O_{34}]^{n-}$, and proposed the resistant mechanism [7–12]. Inoue et al. reported the enhancement of antibacterial activity of beta-lactam antibiotics, oxacillin, by polyoxometalates $(K_6[P_2W_{18}18O_{62}]\cdot14H_2O$, $K_4[SiMo_{12}O_{40}]\cdot3H_2O$, and $K_7[PTi_2W_{10}O_{40}]\cdot6H_2O)$ against methicillin-resistant *Staphylococcus aureus* (MRSA) and vancomycin-resistant *S. aureus* (VRSA) and also proposed a reaction mechanism [13]. Daima et al. studied synergistic antibacterial action of Ag nanoparticles and POMs which were achieved by the physical damage to the bacterial cells [14]. Li and his colleagues showed the short peptides/HSiW nanofibers had antimicrobial activity to the ubiquitous and clinically relevant bacterium *Escherichia coli* [15]. In recent years, there are also many reports about the antibacterial activity of known and new polyoxometalate derivatives to several bacteria including *Escherichia coli*, *Staphylococcus aureus*, *Paenibacillus* sp., *Bacillus subtilis*, *Clavibacter michiganensis*, *Vibrio* sp., *Pseudomonas putida*, *Helicobacter pylori*, *S. typhimurium*, *Streptocoque B* (*S. agalactiae*), *L. acidophilus*, and amebas [3,16–34]. In these reports, the polyoxometalate derivatives are in the form of simple inorganic salts, inorganic-organic hybrids with various organic groups, films, nanofibers, etc. However, the antibacterial activity of these compounds is not satisfactory

according to the reported data. Nevertheless, the emergence of multidrug-resistant bacterial strains which was partially due to the abuse of conventional antibiotics proved that there is an urgent need for novel therapeutic agents. Therefore, synthesizing and exploring new compounds with high antibacterial activity are still a challenging task of chemists and pharmacologist. To achieve this, the study on influence of the composition and structure of compounds on antibacterial activity is very important, which will play an instructional role in synthesizing and exploring new compounds.

This work is about the synthesis of a new poly-oxometalate derivative, $[Cu_2(phen)_4(H_4W_{12}O_{40})]$, and study on the antibacterial activity of several polyoxometalate compounds with different anionic structures including the new compound.

2. Materials and Methods

2.1. Materials and General Methods.
All reagents were purchased commercially and used without further purification. Elemental analyses (C, H, and N) were performed on a Perkin–Elmer 2400 CHN elemental analyzer and that of W and Cu on an ICP–AES analyzer. The IR spectrum was obtained on an Magna-560 FT/IR spectrometer with KBr pellets in the 400–4000 cm^{-1} region. TG analysis was carried out on a DTG-60H thermal analyzer in flowing N_2 with a heating rate of 10°C·min^{-1}. SEM images were recorded on Hitachi S-3400N (Hitachi High-Technologies Europe GmbH, Krefeld, Germany).

2.2. Synthesis.
Synthesis of $[Cu_2(phen)_4(H_4W_{12}O_{40})]$ was modified from our previous report [35]: compound 1 was prepared from reaction of $(NH_4)_6(H_2W_{12}O_{40})\cdot 3H_2O$ (0.1 mmol, 0.30 g), $CuCl_2$ $2H_2O$ (2.0 mmol, 0.34 g), phenanthroline (0.5 mmol, 0.099 g), succinic acid (0.5 mmol, 0.06 g), and 12 mL water. The starting mixture was adjusted to pH = 2.0 by the addition of hydrochloric acid, and the mixture was stirred for 1 h under air. The final solution was transferred to a 25 mL Teflon-lined autoclave and crystallized at 160°C for 96 h. Then, the autoclave was cooled at the rate of 10°C·h^{-1} to room temperature. The resulting green stripe crystals were filtered off, washed with distilled water, and air-dried. Good-quality crystals were sealed for structural determination and further characterization. Elemental analysis calcd for $C_{48}H_{32}Cu_2N_2O_{41}W_{12}$ ($Mr = 3710$) C 1.00, H 12.7619, N 2.48, O 20.68, Cu 3.38, P 1.10, W 58.60 (%); found: C 1.10, H 12.39, N 2.41, O 20.56, Cu 3.39, P 1.09, W 59.05 (%). IR(KBr pellet, cm^{-1}): 3500, 3082, 2370, 2298, 2109, 1994, 1628, 1597, 1524, 1335, 1231, 1085, 948, 781, 750, 708, 667, 593, 530 cm^{-1}.

Compounds 2–6 were prepared in accordance with the methods in Refs. [36–39] and characterized by the IR spectrograph and TGA.

2.3. X-Ray Crystallography.
The X-ray diffraction data of compound 1 were collected on a Bruker Smart Apex II diffractometer with graphite monochromatic Mo Kα radiation (λ = 0.710 73 Å) at 293 K with ω scans (Table 1).

TABLE 1: Crystal data and structure refinements for compound 1.

Formula	$C_{48}H_{32}Cu_2N_8O_{40}W_{12}$
Fw	3710
Crystal system	Monoclinic
Space group	P21/c
a/Å	26.1828(15)
b/Å	11.84219(7)
c/Å	23.3996(13)
α/°	90.00
β/°	113.74(2)
γ/°	90.00
V/Å^3	6641.2(7)
Z	4
D_c/g·cm^{-3}	3.711
F(000)	6600
μ/mm^{-1}	21.419
R_{int}	0.0932
Refine number of reflns/parameters/restraints	13661/991/54
R_factor_all/[$I > 2sigma(I)$]	0.0871/0.0456
wR_factor_ref/[$I > 2sigma(I)$]	0.0857/0.0745
Goodness of fit	0.954

Multiscan absorption corrections were applied. The structures were solved by direct methods and refined by full matrix least-squares on F^2 using the SHELXTL crystallographic software package [40]. The positions of hydrogen atoms on the carbon atoms were calculated theoretically. Crystal data and structure refinements for compound 1 are presented in Table 1. Cu-O and Cu-N bond lengths are listed in Table 2. CCDC-1487664 for 1 contains the supplementary crystallographic data for this paper. These data can be obtained free of charge from The Cambridge Crystallographic Data Centre via http://www.ccdc.cam.ac.uk/data_request/cif.

2.4. Antibacterial Experiments.
All the isolated bacterial strains were achieved by colony formation on selective salt agar plates containing 6 mg/mL oxacillin. All bacterial strains were stored at −80°C and routinely grown at 37°C. *Staphylococcus aureus* (YB57), *Enterococcus faecalis* (FA2 and FA3), and *Enterococcus faecium* (SA2 and SA3) strains were cultured in brain heart infusion (BHI) broth, while *Staphylococcus aureus* (USA300), *Acinetobacter baumannii* (ABC3), and *Streptococcus pneumoniae* (SP) were cultured in the Luria-Bertani (LB) medium. The polyoxometalates were tested for their antibacterial activities against eight different bacterial strains by the observation of the OD value of culture media. Briefly, bacterial cells were washed and resuspended in sterile PBS, and the colony count was determined. The different polyoxometalates were added to the bacterial suspension (final concentration, 1 mg/mL), and the mixture was incubated overnight at 37°C. The colony count was determined again. Enzyme activity *in vitro* was expressed as the CFU reduction. As a negative control, the bacterial strains were treated with the elution buffer under the same conditions. The results are listed in Table 3.

Table 2: Cu-O and Cu-N bond lengths (Å) in **1**.

Bond	Length	Bond	Length
Cu1 N1	2.214(11)	Cu2 N5	1.960(12)
Cu1 N2	1.990(10)	Cu2 N9	2.038(12)
Cu1 N3	1.996(13)	Cu2 N7	1.965(12)
Cu1 N4	1.991(11)	Cu2 N8	2.168(12)
Cu1 O7	2.045(10)	Cu2 O38	2.217(8)

2.5. Scanning Electron Microscopy. Scanning electron microscopy (SEM) was performed to assess the activity of different polyoxometalates on the bacterial strains *in vitro*. The *Staphylococcus aureus* strains USA300 were grown to the exponential growth phase (an OD 600 nm value of 0.6) in the BHI broth at 37°C with shaking at 200 rpm. The bacteria were collected and washed three times (5,000 × g for 1 min at 4°C) with PBS. Different formulations were separately added to *S. aureus* suspensions. Bacterial lysates were harvested by centrifugation (1,100 × g for 1 min) at different time points. Then, the bacterial lysates were fixed with glutaraldehyde and were dehydrated and freeze-dried for SEM.

3. Results and Discussion

3.1. Crystal Structure of 1. The asymmetric unit of compound **1** consists of one Keggin anion $[H_4W_{12}O_{40}]^{6-}$, two Cu^{2+} ions, and four phen molecules. The $[H_4W_{12}O_{40}]^{6-}$ anion (Figure 1) contains four edge-shared W_3O_{13} units which combine together through corner-shared linkage. W–O bonds can be classified into three sets: W–O_t (terminal oxygen atoms) with distances of 1.683(12)–1.740(12) Å, W–O_b (bridging oxygen atoms) with distances of 1.847(12)–2.010(14) Å and W–O_c (central oxygen atoms) with distances of 2.174(12)–2.396(13) Å. That is, the WO_6 octahedra are all distorted. The Keggin anion acts as a bidentate ligand bonding two Cu^{2+} ions (Cu1 and Cu2) with one terminal oxygen atom and one bridge oxygen atom. One W-O_t bond was elongated (1.740(12) Å) due to the coordination of the terminal oxygen atom to Cu ion. Such a POM anion is also called as decorated Keggin anion (Figure 1), very similar to the decoration we reported previously [35].

Two Cu^{2+} ions are all five-coordinated. Cu1 ion displays in a square prism geometry, and the geometry of Cu2 ion is better to be described as triangle bipyramid. The donor atoms bonding to Cu ions come from two phen molecules with chelating coordination mode and the Keggin anion, forming a complex fragment $\{Cu(phen)_2\}^{2+}$ (Figure 1). Cu-O and Cu-N bond lengths are listed in Table 2. As shown in Table 2, the long bonds belong to the atoms at axial site for Cu1 and triangle plane for Cu2 (Figure S1), resulting from their environment in the crystal. Devi et al. [41] had reported a similar cluster $[\{Cu(phen)2\}2(H2W12O40)]^{2-\cdot}$ in $[\{Cu(phen)2\}4\{H2W12O40\}]$ $[\{Cu(phen)2\}2\{H2W12O40\}]\cdot$ 3H2O, in which one Cu ion is six-coordinated, different from that of this new compound. The neutral molecules are assembled into three dimensional architecture through CH···O hydrogen bonds (Table S2) and intermolecular interaction force (Figure S2).

Table 3: Antibacterial activities of compounds **1–6**.

Type	Code	Compound	Concentration	Bacterial strains
I	1	$[\{Cu(phen)_2\}_2(H_4W_{12}O_{40})]$	1 mg/mL	FA2
				ABC3,
				FA2,
	2	$[Cu(phen)(H_2O)(Mo_3O_{10})]$	1 mg/mL	FA3, YB57, USA300
II	3	$K_5PW_{11}TiO_{40}\cdot14H_2O$	1 mg/mL	YB57, USA300
III	4	$Na_7CeW_{10}O_{35}\cdot26H_2O$	1 mg/mL	SA5, SA1, SP, USA300
	5	$K_{13}[La(SiW_{11}O_{39})_2]\cdot26H_2O$	1 mg/mL	YB57, USA300
IV	6	$K_{13}[Ce(SiW_{11}O_{39})_2]\cdot 26H_2O$	1 mg/mL	SA5, SA1, SP, USA300

3.2. Characterization of 1. The IR spectrum (Figure S3) of **1** shows the vibration absorption bands of CH bond in 3080 cm^{-1} and of C-C and N-C bonds of phen ring in 1614–1137 cm^{-1}. The vibration absorption bands of compound **1** at 952, 877, 846, and 740 cm^{-1} should be ascribed to the asymmetric stretching vibrations of W-O_d, W-O_b-W, and W-O_c-W bonds, respectively, consistent with that in Ref. [42]. The TG curve of **1** is shown in Figure S4. Compound **1** is stable below 400°C and then decomposes until 600°C. The lost weight of 20.17% is consistent with the calculated one (20.38% for $2H_2O$ and 4phen), confirming the chemical formula obtained from elemental analysis and structure analysis.

3.3. Antibacterial Activity of 1–6. The compounds **1–6** used in antibacterial experiments can be divided into four kinds. **1** and **2** are inorganic-organic hybrids with phenanthroline, and **3** is a mono-substituted Keggin-type compound in which Ti atom occupies one of twelve sites. **4** is a complex of mono-lacunaria Lindquist anion and lanthanides. **5** and **6** are complexes of mono-lacunaria Keggin anions and lanthanides. From Table 3, it can be seen that (1) the new compound **1** is active only to bacterial strains FA2. (2) The compound of molybdenum, **2**, has a wider antibacterial spectrum than that of tungsten (**1**, **3**, **4**, **5**, **6**). (3) The anionic structure has less influence on antibacterial activity. (4) The compounds with cerium element (**4**, **6**) show better antibacterial activity than others.

SEM technique was used to explore the interaction of polyoxometalates with the bacterial strains. SEM images (Figure 2) show the surface morphology of *Staphylococcus aureus* strains USA300 untreated (Figure 2(a)) and treated with **3**, **4**, **5**, and **6** (Figures 2(b)–2(e)). From Figure 2, it can be seen that the surface morphology of *Staphylococcus aureus* strains USA300 treated with polyoxometalates (Figures 2(b)–2(e)) has changed obviously compared with that of untreated one (Figure 2(a)) from smooth globular form to chapping oblate spheroid. The degree of changes in the surface morphology indicates the antibacterial activity of
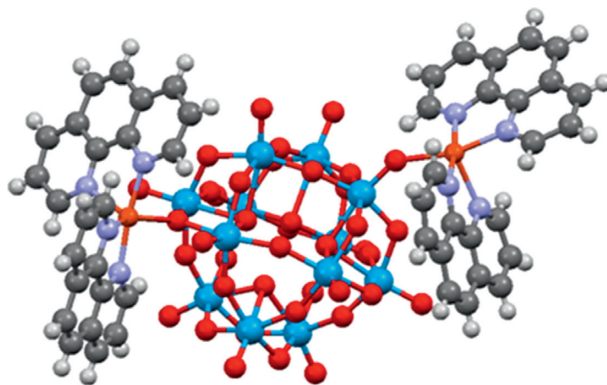
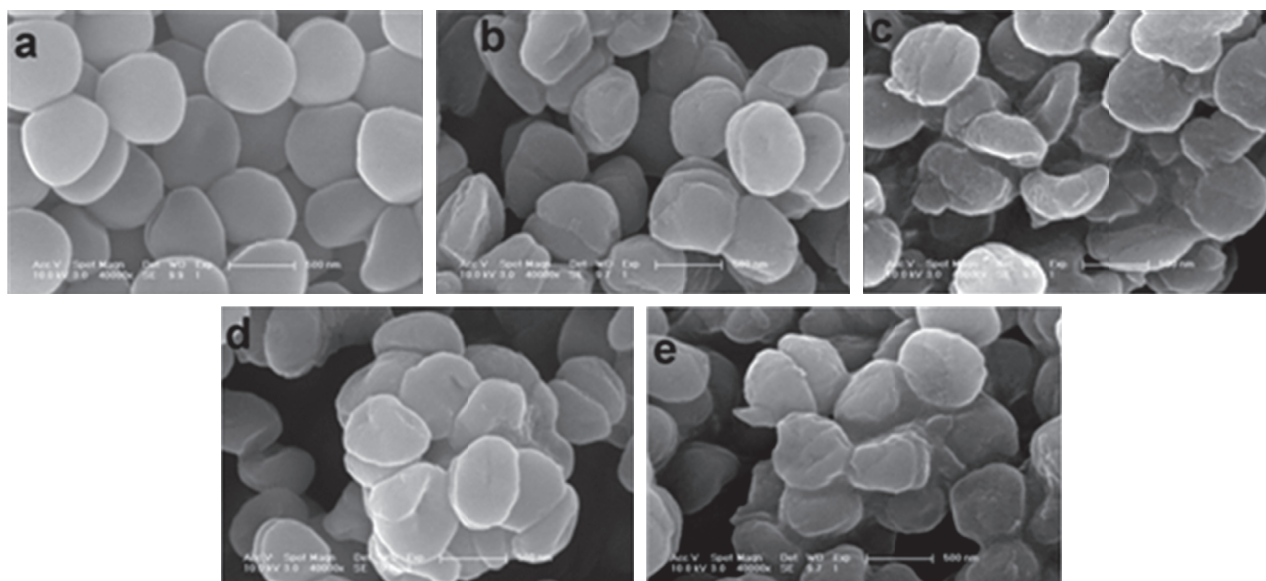FIGURE 1: Ball-stick representation of the decorated Keggin anion in **1**.

FIGURE 2: SEM images of *Staphylococcus aureus* strains USA300 untreated (a) and treated with **3** (b), **4** (c), **5** (d), and **6** (e).

polyoxometalates. So, a sequence of the activity of polyoxometalates was given according to Figure 2, **4** ≈ **6** > **5** > **3**. That is, the compounds with cerium element (**4**, **6**) have better antibacterial activity than others.

4. Conclusion

The bioactivity of polyoxometalates has been known for many years but still has large space to explore. The results of this work on the antibacterial activity of polyoxometalates including the new compound show that antibacterial activity of the compounds is more relative with their component element than with anionic structure, which means that exploration of antibacterial materials should focus on the choice of elements.

In this work, the compounds with Ce elements have better antibacterial activity. So, synthesizing compounds with other lanthanide elements and other compounds with cerium element and examining their antibacterial activity as well as exploring the reaction mechanism of Ce compounds need further investigations.

Data Availability

The data used to support the findings of this study are included within the article.

Conflicts of Interest

The authors declare no conflicts of interest.

Authors' Contributions

Jingmin Gu and Lei Zhang contributed equally to this article.

Acknowledgments

Wali Khan University, Mardan, Pakistan, for generously providing *Enterococcus faecium* strains (SA2 and SA3) and *Streptococcus pneumoniae* strain (SP).

Supplementary Materials

Figure S1: coordination geometries of Cu ions; Figure S2: stacking representation of **1** from three directions of (A) *a*-axis, (B) *b*-axis, and (C) *c*-axis; Figure S3: IR spectrum of **1**; Figure S4: TG plot of **1** in 0-600℃; Table S1: W-O bond lengths (Å); Table S2: CH⋯O hydrogen bonds in **1**. (*Supplementary Materials*)

References

[1] J. T. Rhule, C. L. Hill, and D. A. Judd, "Polyoxometalates in medicine," *Chemical Reviews*, vol. 98, no. 1, pp. 327–357, 1998.

[2] A. Seko, T. Yamase, and K. Yamashita, "Polyoxometalates as effective inhibitors for sialyl- and sulfotransferases," *Journal of Inorganic Biochemistry*, vol. 103, no. 7, pp. 1061–1066, 2009.

[3] M. Inoue, K. Segawa, S. Matsunaga et al., "Antibacterial activity of highly negative charged polyoxotungstates, K27 [KAs4W40O140] and K18[KSb9W21O86], and Keggin-structural polyoxotungstates against *Helicobacter pylori*," *Journal of Inorganic Biochemistry*, vol. 99, no. 5, pp. 1023–1031, 2005.

[4] T. L. Turner, V. H. Nguyen, C. C. McLauchlan et al., "Inhibitory effects of decavanadate on several enzymes and *Leishmania tarentolae* in vitro," *Journal of Inorganic Biochemistry*, vol. 108, pp. 96–104, 2012.

[5] Y. Qi, Y. Xiang, J. Wang et al., "Inhibition of hepatitis C virus infection by polyoxometalates," *Antiviral Research*, vol. 100, no. 2, pp. 392–398, 2013.

[6] K. Nomiya, H. Torii, T. Hasegawa et al., "Insulin mimetic effect of a tungstate cluster. Effect of oral administration of homo-polyoxotungstates and vanadium-substituted polyoxotungstates on blood glucose level of STZ mice," *Journal of Inorganic Biochemistry*, vol. 86, no. 4, pp. 657–667, 2001.

[7] T. Yamase, N. Fukuda, and Y. Tajima, "Synergistic effect of polyoxotungstates in combination with beta-lactam antibiotics on antibacterial activity against methicillin-resistant *Staphylococcus aureus*," *Biological and Pharmaceutical Bulletin*, vol. 19, no. 3, pp. 459–465, 1996.

[8] Y. Tajima, "Purification of a factor that enhances the antibacterial activity of beta-lactams against methicillin-resistant *Staphylococcus aureus*: its identification as undecaphosphotungstate," *Journal of Inorganic Biochemistry*, vol. 68, no. 2, pp. 93–99, 1997.

[9] Y. Tajima, "Lacunary-substituted undecatungstosilicates sensitize methicillin-resistant Staphylococcus aureus to beta-lactams," *Biological and Pharmaceutical Bulletin*, vol. 24, no. 9, pp. 1079–1084, 2001.

[10] Y. Tajima, "The effects of tungstophosphate and tungstosilicate on various stress promoters transformed in Escherichia coli," *Journal of Inorganic Biochemistry*, vol. 94, no. 1-2, pp. 155–160, 2003.

[11] Y. Tajima, "Effects of tungstosilicate on strains of methicillin-resistant *Staphylococcus aureus* with unique resistant mechanisms," *Microbiology and Immunology*, vol. 47, no. 3, pp. 207–212, 2003.

[12] Y. Tajima, "Polyoxotungstates reduce the beta-lactam resistance of methicillin-resistant *Staphylococcus aureus*," *Mini-Reviews in Medicinal Chemistry*, vol. 5, no. 3, pp. 255–268, 2005.

[13] M. Inoue, T. Suzuki, Y. Fujita et al., "Enhancement of antibacterial activity of beta-lactam antibiotics by [P2W18O62]6-, [SiMo12O40]4-, and [PTi2W10O40]7- against methicillin-resistant and vancomycin-resistant *Staphylococcus aureus*," *Journal of Inorganic Biochemistry*, vol. 100, no. 7, pp. 1225–1233, 2006.

[14] H. K. Daima, P. R. Selvakannan, A. E. Kandjani et al., "Synergistic influence of polyoxometalate surface corona towards enhancing the antibacterial performance of tyrosine-capped Ag nanoparticles," *Nanoscale*, vol. 6, no. 2, pp. 758–765, 2014.

[15] J. Li, Z. Chen, M. Zhou et al., "Polyoxometalate-driven self-assembly of short peptides into multivalent nanofibers with enhanced antibacterial activity," *Angewandte Chemie International Edition in English*, vol. 55, no. 7, pp. 2592–2595, 2016.

[16] Y. Feng, Z. Han, J. Peng et al., "Fabrication and characterization of multilayer films based on Keggin-type polyoxometalate and chitosan," *Materials Letters*, vol. 60, no. 13, pp. 1588–1593, 2006.

[17] K. H. Wu, P. Y. Yu, C. C. Yang et al., "Preparation and characterization of polyoxometalate-modified poly(vinyl alcohol)/polyethyleneimine hybrids as a chemical and biological self-detoxifying material," *Polymer Degradation and Stability*, vol. 94, no. 9, pp. 1411–1418, 2009.

[18] C. G. Feng, Y. D. Xiong, and X. Liu, "Synthesis, spectroscopy and antibacterial activity of supermolecular compounds of organotitanium substituted heteropolytungstates containing 8-quinolinol," *Guang Pu Xue Yu Guang Pu Fen Xi*, vol. 31, no. 5, pp. 1153–1160, 2011.

[19] S. Gao, Z. Wu, D. Pan et al., "Preparation and characterization of polyoxometalate–Ag nanoparticles composite multilayer films," *Thin Solid Films*, vol. 519, no. 7, pp. 2317–2322, 2011.

[20] R. Raza, A. Matin, S. Sarwar et al., "Polyoxometalates as potent and selective inhibitors of alkaline phosphatases with profound anticancer and amoebicidal activities," *Dalton Transactions*, vol. 41, no. 47, pp. 14329–14336, 2012.

[21] J. He, H. Pang, W. Wang et al., "Uniform M3PMo12O40.nH2O (M = NH4+, K+, Cs+) rhombic dodecahedral nanocrystals for effective antibacterial agents," *Dalton Transactions*, vol. 42, no. 44, pp. 15637–15644, 2013.

[22] H. K. Daima, P. R. Selvakannan, R. Shukla et al., "Fine-tuning the antimicrobial profile of biocompatible gold nanoparticles by sequential surface functionalization using polyoxometalates and lysine," *PLoS One*, vol. 8, no. 10, Article ID e79676, 2013.

[23] X. Yu, C. Chen, J. Peng et al., "Antibacterial-active multilayer films composed of polyoxometalate and Methyl Violet: fabrication, characterization and properties," *Thin Solid Films*, vol. 571, pp. 69–74, 2014.

[24] A. Maalaoui, A. Hajsalem, N. Ratel-Ramond et al., "Synthesis, characterization and antibacterial activity of a novel photoluminescent nb-substituted lindqvist polyoxotungstate based organic cation," *Journal of Cluster Science*, vol. 25, no. 6, pp. 1525–1539, 2014.

[25] G. Fiorani, O. Saoncella, P. Kaner et al., "Chitosan-polyoxometalate nanocomposites: synthesis, characterization and application as antimicrobial agents," *Journal of Cluster Science*, vol. 25, no. 3, pp. 839–854, 2014.

[26] L. Grama, A. Man, D.-L. Muntean et al., "Antibacterial activity of some saturated polyoxotungstates," *Romanian Journal of Laboratory Medicine*, vol. 22, no. 1, pp. 111–118, 2014.

[27] L. De Matteis, S. G. Mitchell, and M. Jesús, "Supramolecular antimicrobial capsules assembled from polyoxometalates and

chitosan," *Journal of Materials Chemistry B*, vol. 2, no. 41, pp. 7114–7117, 2014.

[28] H. Liu, Y.-L. Zou, L. Zhang et al., "Polyoxometalate cobalt–gatifloxacin complex with DNA binding and antibacterial activity," *Journal of Coordination Chemistry*, vol. 67, no. 13, pp. 2257–2270, 2014.

[29] P. Yang, B. S. Bassil, Z. Lin et al., "Organoantimony(III)-containing tungstoarsenates(III): from controlled assembly to biological activity," *Chemistry*, vol. 21, no. 44, pp. 15600–15606, 2015.

[30] X.-X. Lu, Y.-H. Luo, C. Lu et al., "Assembly of three new POM-based Ag(I) coordination polymers with antibacterial and photocatalytic properties," *Journal of Solid State Chemistry*, vol. 232, pp. 123–130, 2015.

[31] P. Gull and A. A. Hashmi, "Biological activity studies on metal complexes of macrocyclic schiff base ligand: synthesis and spectroscopic characterization," *Journal of the Brazilian Chemical Society*, vol. 26, no. 7, pp. 1331–1337, 2015.

[32] P. Yang, Z. Lin, B. S. Bassil et al., "Tetra-antimony(III)-bridged 18-tungsto-2-arsenates(V), [(LSb(III))4(A-alpha-As(V)W9O34)2](10-) (L = ph, OH): turning bioactivity on and off by ligand substitution," *Inorganic Chemistry*, vol. 55, no. 8, pp. 3718–3720, 2016.

[33] W. W. Ayass, T. Fodor, Z. Lin et al., "Synthesis, structure, and antibacterial activity of a thallium(III)-containing polyoxometalate, [Tl2{B-beta-SiW8O30(OH)}2](12)," *Inorganic Chemistry*, vol. 55, no. 20, pp. 10118–10121, 2016.

[34] S. Balici, M. Niculae, E. Pall et al., "Antibiotic-like behaviour of polyoxometalates in vitro comparative study: seven polyoxotungstates-nine antibiotics against gram-positive and gram-negative bacteria," *Revista de Chimie*, vol. 67, no. 3, pp. 485–490, 2016.

[35] H. Wang, H. Liu, T. Shi et al., "Decorated Dawson anion by two different complex fragments of phenanthroline and isonicotinic acid: synthesis and properties," *Journal of Cluster Science*, vol. 28, no. 3, pp. 1041–1049, 2017.

[36] H.-Y. Wang, T. Shi, and Y.-G. Chen, "Molybdenum-oxygen anionic chain grafted by Cu-phen complex. Synthesis, crystal structure and properties," *Inorganic Chemistry Communications*, vol. 70, pp. 201–204, 2016.

[37] O. A. Kholdeeva, T. A. Trubitsina, G. M. Maksimov et al., "Synthesis, characterization, and reactivity of Ti(IV)-monosubstituted Keggin polyoxometalates," *Inorganic Chemistry*, vol. 44, no. 5, pp. 1635–1642, 2005.

[38] R. Peacock and T. Weakley, "Heteropolytungstate complexes of the lanthanide elements. Part I. Preparation and reactions," *Journal of the Chemical Society A: Inorganic, Physical, Theoretical*, pp. 1836–1839, 1971.

[39] S. Zubairi, S. Ifzal, and A. Malik, "Heteropoly complexes of lanthanum with unsaturated heteropolytungstate ligands," *Inorganica Chimica Acta*, vol. 22, pp. L29–L30, 1977.

[40] G. Sheldrick, *SHELXL97, Program for Crystal Structure Refinement*, University of Göttingen, Göttingen, Germany, 1997.

[41] R. N. Devi, E. Burkholder, and J. Zubieta, "Hydrothermal synthesis of polyoxotungstate clusters, surface-modified with M (II)-organonitrogen subunits," *Inorganica Chimica Acta*, vol. 348, pp. 150–156, 2003.

[42] M. Asami, H. Ichida, and Y. Sasaki, "The structure of hexakis (tetramethylammonium) dihydrogendodecatungstate enneahydrate,[(CH3) 4N] 6 [H2W12O40] 9H2O," *Acta Crystallographica Section C: Crystal Structure Communications*, vol. 40, no. 1, pp. 35–37, 1984.